Arch. Metall. Mater. **69** (2024), 1, 217-221

DOI: https://doi.org/10.24425/amm.2024.147811

FEI HUANG[1*]

THE EFFECT OF ADDITION AMOUNT OF CHROMIUM IRON ON THE BONDING STRENGTH BETWEEN ALLOY STEEL SURFACING LAYER AND STEEL BASE METAL

Fe-C-Cr-Nb alloy steel surfacing layers with different contents of C and Cr were prepared on 45 steel base metal by self-shielded flux-cored wires with distinct amounts of high carbon chromium iron addition and melt arc surfacing. The composition and microstructure changes of the surfacing layer were tested and analyzed. The surfacing test plate was processed into a pulling specimen, and the bonding strength between the surfacing layer and the 45 steel base metal was tested with a self-designed pulling test method. The fracture location of the pulling specimen and fracture characteristics were observed by a metallurgical microscope and a scanning electron microscope. The result shows that with the increase of the amount of high carbon chromium iron added to flux-cored welding wire, the content of C and Cr in the surfacing layer increases, and the NbC hard phase disperses. The microstructure of the steel matrix changes from mixed martensite + residual austenite to high carbon martensite + residual austenite, and then independent austenite appears. The hardness of the surfacing layer first increases and then decreases. The bonding strength between the surfacing alloy and the 45 steel base metal first decreases and then increases, and the fracture location is at the bottom of the surfacing layer or the fusion zone with mostly quasi-cleavage characteristics. When the additional amount of high carbon chromium iron reaches 13%, thee pulling specimen exhibits significant deformation with the highest bonding strength, and the fracture is close to the fusion line, where there are numerous tearing edges and shallow dimples.

Keywords: Fe-C Cr Nb Alloy Steel; Bonding Strength; Arc Surfacing; Pulling Test Method; High Carbon Chromium Iron

1. Introduction

The failure mode of the main components in plenty of equipment is wear and tear for industries such as cement, electricity, and mining. The main processes of cement production include the crushing and calcination of ore raw materials, as well as the grinding of clinker, which can be summarized as “two grindings and one burning”. The main equipment of the cement grinding system is a vertical roller mill and a roller press. Various wear-resistant surfacing materials and welding processes are widely used in the manufacturing and repair of its main components [1]. The failure mode of the grinding table and roller of a vertical roller mill is abrasive wear, which is mainly subjected to grinding pressure, Fe-C-Cr-Nb+X (X = Ti, B, V, etc.) alloy cast iron surfacing material with NbC and M_7C_3 carbides can be used [2-7]. The main component of the roller press is the extrusion roller, with a patterned working layer on the surface. During operation, it bears alternating loads and fatigue cracks are prone to initiate and expand between the welding layers and the interface between the welding layer and the base metal, leading to local peeling of the wear-resistant layer and early failure. The practice has proven that alloy cast iron type surfacing materials are not suitable for extrusion rolls, and Fe-C-Cr-Nb alloy steel surfacing materials with good fatigue wear resistance can be used [8]. Generally speaking, under the same load, the bonding strength between the surfacing layer and the base metal is higher, the plasticity and toughness of the interface area material will be better, and the ability to resist fatigue failure will be stronger accordingly. Therefore, studying the influence of metallurgical and process factors on the bonding strength between the surfacing layer and the base metal has theoretical significance and practical value for regulating the fatigue wear resistance of the extrusion roller.

In this paper, Fe-C-Cr-Nb alloy steel surfacing layers with different contents of C and Cr were prepared on 45 steel base metal by self-shielded flux-cored wires with different amounts of high carbon chromium iron addition and melt arc surfacing. The bonding strength between the surfacing layer and the 45 steel base metal was tested with a self-designed pulling test method and the fracture characteristics were observed simultaneously.

[1] HIGH SPEED RAILWAY COMPREHENSIVE TECHNICAL COLLEGE, JILIN RAILWAY TECHNOLOGY COLLEGE, JILIN, 132299, CHINA

* Corresponding author: huangfei80616@126.com

2. Test materials, methods, and equipment

Fe-C-Cr-Nb alloy steel surfacing layers with different contents of C and Cr were prepared on 45 steel base metal by self-shielded flux-cored wires with different amounts of high carbon chromium iron addition and melt arc surfacing. Welding wire diameter 2.8 mm, base metal 200×120×25 mm. Fix the welding gun on the walking car with the NBC-630 inverter welding machine, and after arc striking, the car drives the welding gun to automatically weld on the surface of the base metal, with a total of 3 layers of welding. The welding parameters are shown in TABLE 1.

Composition analysis and metallographic samples were prepared by cutting the surfacing test plate with an electric spark. The composition analysis samples were tested by ARL 4460 photoelectric direct reading spectrometer, the surface hardness of the surfacing layer was tested by HR-150A hardness tester and the microstructure of the surfacing layer and the area near the fusion line was observed and recorded by Axio Scope. Cut and pull the test piece according to Fig. 1, and smooth, polish the surface, and make corrosion treatment. Pulling testing is made by a WQ-4100 tensile testing machine.

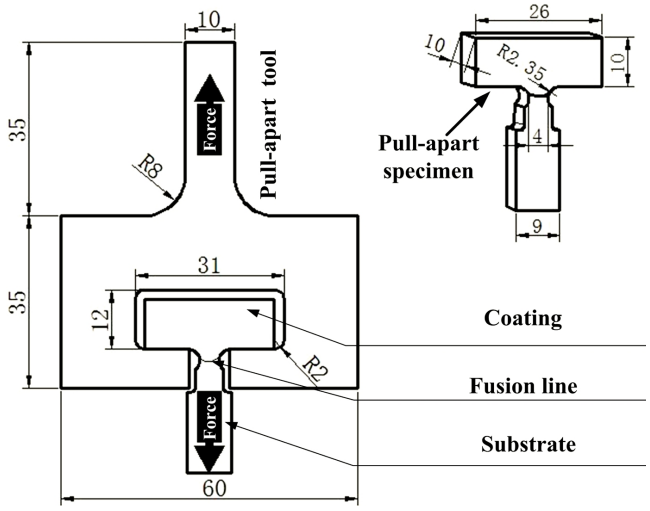

Fig. 1. Pulling Specimen and Schematic Diagram of Pulling Test

Assemble the pulling specimen and fixture according to Fig. 1, and use the lower clamp of the testing machine to center and clamp the pull-down end of the pulling specimen, while the upper clamp aligns and clamps the upper lifting end of the fixture. Record the maximum lifting force and measure the actual fracture area to obtain the bonding strength between the surfacing layer and the base metal. After the pulling test, the fracture location and characteristics of the pulling specimen were analyzed by a metallurgical microscope and a JXA-840 scanning electron microscope.

3. Test results and analysis

3.1. Composition, hardness, and microstructure of the surfacing layer

The composition analysis results and macroscopic hardness test results of the different amounts of high carbon chromium iron addition and melt arc surfacing are shown in TABLE 2. With the increase of the amount of high carbon chromium iron addition, the C and Cr contents in Fe-C-Cr-Nb surfacing alloy steel correspondingly increase, with the C content increasing from 1.07% to 1.48% and the Cr content increasing from 0.08% to 3.53%. In addition, the surfacing layer contains about 4.7% Nb and about 1.3% Mn elements with little variation in the content of Nb, Mn, and other elements. The hardness of the surfacing layer increased from 45.2 HRC to 62.7 HRC and gradually decreased to 47.1 HRC.

The typical microstructure of the Fe-C Cr Nb alloy steel surfacing layer is shown in Fig. 2. When high carbon chromium iron is not added to the welding wire, C content will be high because of the addition of a certain amount of graphite; and the microstructure is mainly composed of mixed martensite, residual austenite, and NbC particles, as shown in Fig. 2a.

TABLE 1

Welding Process Parameters for Surfacing

Current I/A	Voltage U/V	Welding speed V/(cm·min^{-1})	Electrode extension L/mm	Interlayer temperature T/°C	Postweld state
320~350	27.5~28.5	42	15~20	200	Air-cooling

TABLE 2

Composition of Surfacing Alloy with Different Addition Levels of High Carbon Chromium Iron Welding Wire (wt.%)

Welding wire/ specimen number	High Carbon Chromium Iron added amount (wt.%)	C	Cr	Si	Mn	S	P	Nb	Ni	Al	Fe	Hardness (HRC)
1#	0%	1.07	0.08	0.50	1.33	0.008	0.023	4.55	0.09	0.009	Bal.	45.2
2#	2.5%	1.25	0.77	0.53	1.31	0.013	0.019	4.63	0.10	0.014	Bal.	62.7
3#	5.0%	1.29	1.33	0.53	1.32	0.009	0.027	4.62	0.09	0.013	Bal.	61.4
4#	7.5%	1.32	2.00	0.55	1.23	0.009	0.026	4.80	0.09	0.014	Bal.	58.6
5#	10%	1.41	2.61	0.55	1.31	0.012	0.026	4.98	0.11	0.012	Bal.	58.2
6#	13%	1.48	3.53	0.55	1.30	0.009	0.024	4.72	0.09	0.013	Bal.	47.1

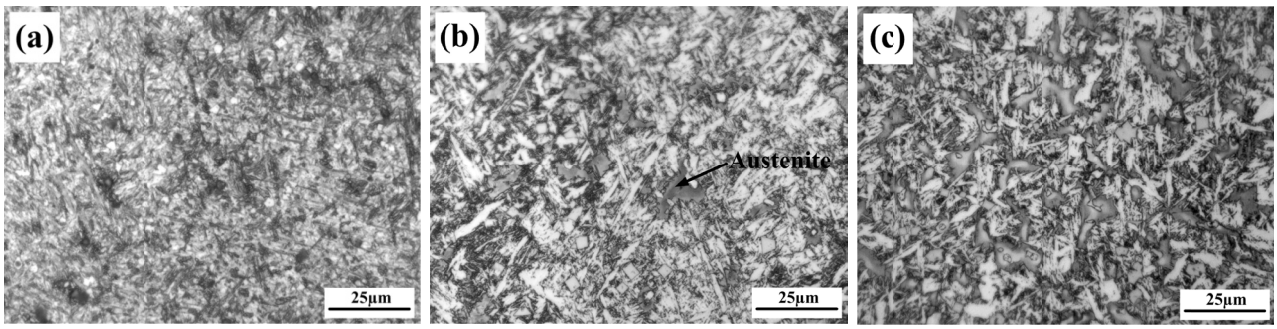

Fig. 2. Typical Micro-structure of Fe-C-Cr-Nb Alloy Steel Surfacing Layer (a) 1#, (b) 4#, (c) 6#

Due to the high content of Nb in the surfacing alloy, NbC crystal nuclei are first formed and grow in the liquid molten pool, which consumes a large amount of C, resulting in a lower content of C in the high-temperature austenite after solidification. Owing to the fast cooling rate, a large amount of low-carbon martensite is formed in the matrix of Fe-C-Cr-Nb surfacing alloy steel, with only a small amount of high-carbon martensite, resulting in a lower hardness of the surfacing layer. C and Cr content increases in the surfacing layer with the addition of a small amount of high carbon chromium iron to the welding wire. After the precipitation of NbC particles, the C content in the alloy steel matrix is still high. In addition, the effect of Cr on improving the hardenability forms a microstructure mainly composed of high carbon martensite, and the hardness of the surfacing layer is significantly increased, reaching 62.7HRC. Subsequently, as the addition of high carbon chromium iron continued to increase, the C and Cr content in the Fe-C-Cr-Nb alloy steel surfacing layer correspondingly increased. A small amount of smooth block-like independent austenite was observed in the surfacing layer of the 4# test plate, resulting in a decrease in hardness. In the surfacing layer of the 6# test plate, there is more blocky independent austenite, forming a microstructure of martensite plus residual austenite+more independent austenite+NbC particles, resulting in a decrease in hardness to 47.1HRC.

Fig. 3 shows the microstructure near the fusion zone. The matrix structure of the fusion zone of sample 1# is coarse needle-like martensite+residual austenite, and the bottom of the surfacing layer above it is a mixed martensite+residual austenite structure, with NbC small particles dispersed on the matrix. The fusion zone of the 4# surfacing alloy is composed of fine needle-like martensite+residual austenite+NbC particle structure, and the bottom of the surfacing layer above it is composed of relatively developed needle-like martensite+a small amount of residual austenite+larger NbC particle structure. There is only a small amount of fine needle-like martensite in the fusion zone of the 6# surfacing alloy, and there exist some hidden needle martensite and residual austenite in the light gray area, as well as many independent austenite and NbC particles.

3.2. Bonding strength between the surfacing layer and 45 steel base metal, and fracture characteristics of the specimen

The pulling test method was used to test the bonding strength between the surfacing layer prepared with different amounts of high carbon chromium iron flux cored welding wires and the 45 steel base metal. The test results are shown in Fig. 4.

Due to the simultaneous changes in C and Cr content in the surfacing layer, the horizontal axis adopts the amount of high carbon chromium iron added to the welding wire. From Fig. 4, it can be seen that the bonding strength between the surfacing alloy prepared without the addition of high carbon chromium iron and the 45 steel base metal is relatively high, which is 381 MPa. The increase in the amount of high carbon chromium iron addition leads to a decrease in the bonding strength. When the addition amount is 7.5% (specimen #4), the bonding strength between Fe-C-Cr-Nb surfacing alloy and 45 steel base metal is the lowest, at 267 MPa. As the addition of high-carbon chromium iron continues to increase, the bonding strength rapidly rebounds. When the addition of high carbon chromium iron

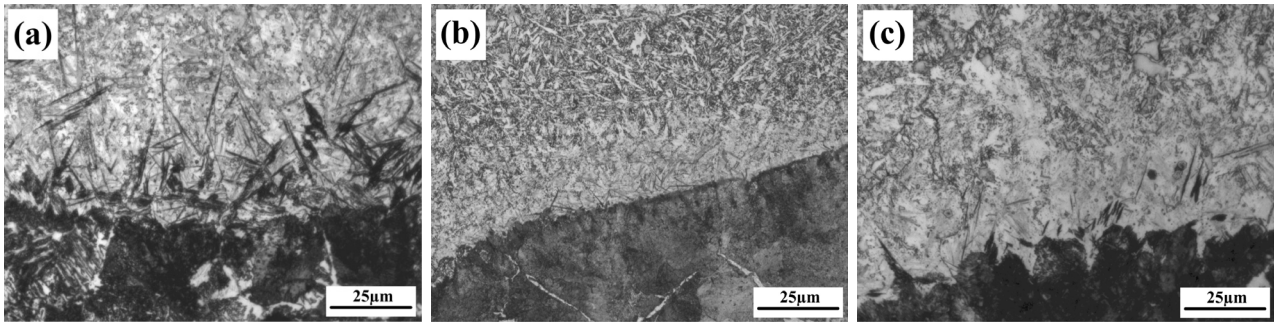

Fig. 3. Micro-structure near the interface between the surfacing layer and the 45 steel base material (a) 1#, (b) 4#, (c) 6#

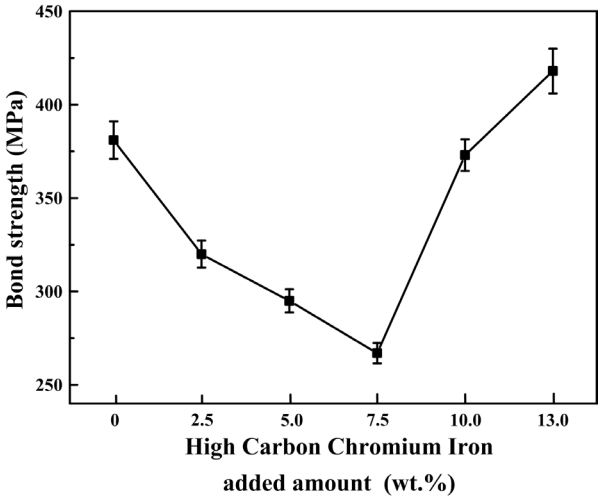

Fig. 4. Bonding strength between surfacing layer prepared by flux-cored welding wire with different amounts of high carbon chromium iron addition and 45 steel base metal

is 13% (specimen 6#), the pulling test piece has the highest bonding strength, which is 418MPa.

Fig. 5 shows the fracture path and characteristics of the 1# pulling specimen. Judging from the fracture path in Fig. 5b, a small amount of deformation and cracks first occurred at the pores in the fusion zone on the right side of the sample during the pulling test, which extended to the left along the fusion zone and the bottom of the surfacing layer, passing through the fusion line locally, and finally forming a mixed fracture path of the bottom of the surfacing layer+fusion zone+fusion line due to the microstructure of the fusion zone mainly consisting of needle-like martensite and NbC particles (see Fig. 3a). The SEM morphology of the fracture is shown in Fig. 5c, and there are many steps and planes with few and small tearing edges, exhibiting quasi-cleavage characteristics. NbC particles are marked with A in the figure by EDS.

Fig. 6 shows the fracture path and characteristics of the 4# pulling specimen. From the analysis of the fracture path in Fig. 6b, the pushed specimen first initiated cracks at the bottom of the surfacing layer near the fusion zone on the left side, then extended to the lower part of the surfacing layer to the right and above, and then zigzagged through the surfacing layer. There was no significant deformation on both sides of the fracture path. The fracture surface in Fig. 6c consists of many steps and small planes, as well as a secondary crack, exhibiting cleavage fracture characteristics.

Fig. 7 shows the fracture path and characteristics of the 6# pulling specimen. There are defects such as pores in the fusion zone and the bottom of the surfacing layer on the right side of the pulling test piece. From Fig. 7b, it can be seen that the fracture path is mainly in the fusion zone near the fusion line, partially entering the bottom of the surfacing layer with uneven and staggered sides. According to the analysis of metal deformation on the fracture path, the bottom metal of the left side of the specimen's surfacing layer first deforms, initiates cracks, and then meanders and expands in the fusion zone and the bottom of the surfacing layer, and then enters the fusion zone near the fusion line, extends to the right gas hole and enters the bottom of the surfacing layer and quickly expands and penetrates the pulling specimen during the pulling process. The microscopic fracture morphology is shown in Fig. 7c, characterized by unevenness, numerous tearing edges, observable blocky particles, and numerous shallow dimples.

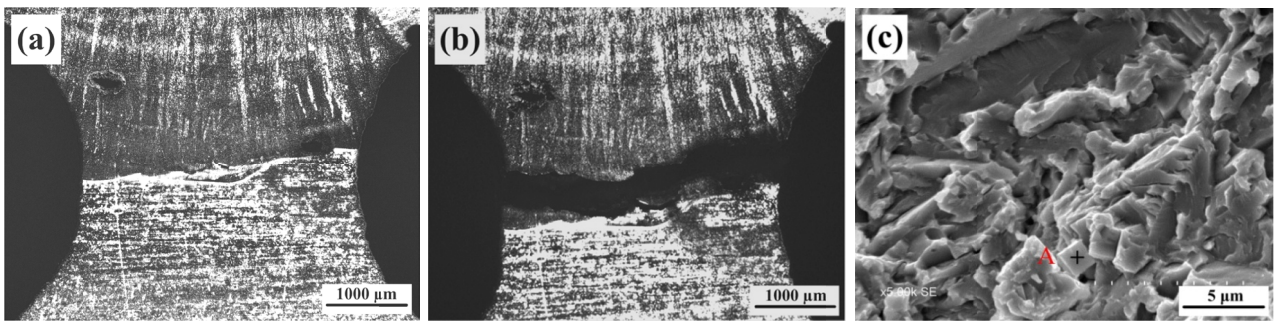

Fig. 5. SEM Image of Fracture Location and Surface of 1# Pulling Sample (a) before pulling test (b) after pulling test (c) SEM image of fractograph

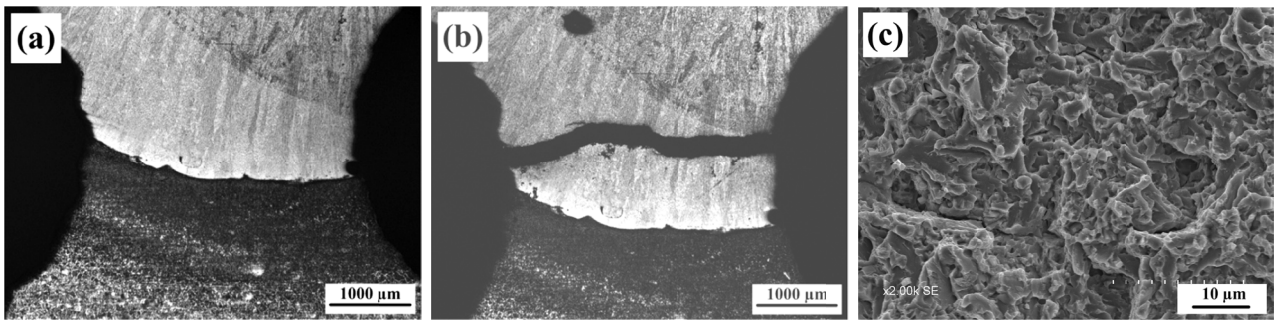

Fig. 6. SEM Image of Fracture Location and Surface of 4# Pulling Sample (a) before pulling test (b) after pulling test (c) SEM image of fractograph

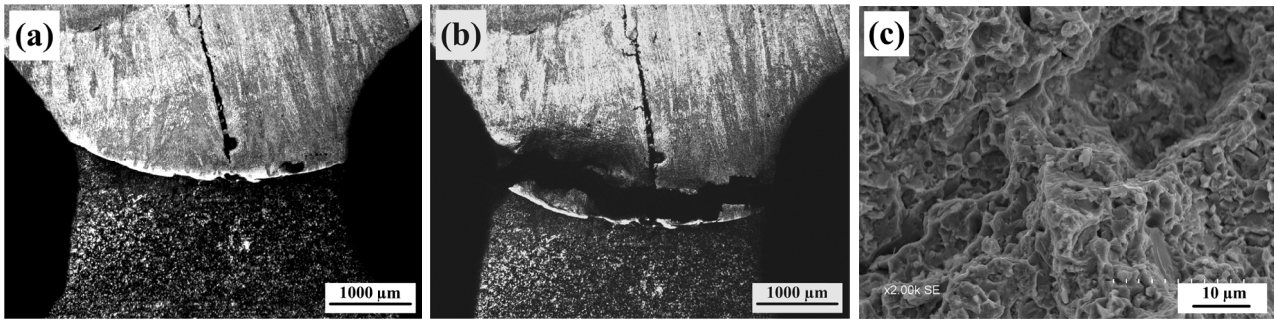

Fig. 7. SEM Image of Fracture Location and Surface of 6# Pulling Sample (a) before pulling test (b) after pulling test (c) SEM image of fractograph

4. Conclusion

The changing amount of high carbon chromium iron added to the self-shielded flux-cored wire changes the C and Cr content in the Fe-C-Cr-Nb alloy steel surfacing layer, as well as alters the microstructure near the surfacing layer and fusion zone correspondingly. The following conclusions were obtained by testing the bonding strength between the surfacing layer and the 45 steel base metal with a self-designed pulling test:

(1) As the amount of high carbon chromium iron added to the welding wire increases, the C and Cr contents in Fe-C-Cr-Nb surfacing alloy steel correspondingly increase. The C content increases from 1.07% to 1.48%, and the Cr content improves from 0.08% to 3.53%. The hardness of the surfacing layer increased from 45.2 HRC to 62.7 HRC and gradually decreased to 47.1 HRC.

(2) When high carbon chromium iron is not added, the microstructure of the surfacing layer is mixed martensite+residual austenite and NbC particles. As the content of C and Cr in the surfacing layer increases, high carbon martensite is formed as the hardness of the surfacing layer significantly increases. Continuing to increase the content of C and Cr, block-like independent austenite with smooth edges appeared in the surfacing layer and continued to increase, forming a microstructure of martensite+residual austenite, independent austenite and NbC particles in the surfacing layer. The microstructure of the area near the fusion zone is similar to that of the surfacing layer.

(3) The bonding strength between the alloy steel surfacing layer prepared with non-added high carbon chromium iron welding wire and the 45 steel base metal is 381 MPa. The pulling specimen extends and cracks along the bottom of the surfacing layer, fusion zone, and fusion line with many quasi-cleavage features of steps and planes on the fracture surface. The addition of high carbon chromium iron reduces the bonding strength. When the addition amount is 7.5%, the bonding strength between the Fe-C-Cr-Nb alloy steel surfacing and the 45 steel base metal is the lowest, which is 267 MPa. Besides, the pulling specimen undergoes brittle fracture at the bottom of the surfacing layer. Increasing the amount of high carbon chromium iron, the bonding strength of the pulling specimen rebounded. When the addition amount was 13%, the local deformation of the pulling test piece was relatively large with bonding strength reaching 418 MPa. The fracture path is close to the fusion line and partially enters the bottom of the surfacing layer, which is uneven and presents many tearing edges as well as shallow dimples.

Funding

The work is supported by the Scientific research project of Education Department of Jilin Province, China (Grant No. JJKH20241159KJ).

REFERENCE

[1] Wei Jianjun, Pan Jian, Huang Zhiquan, et al The application of wear-resistant surfacing materials in China's cement industry [J]. China Surface Engineering **19** (3), 9-13 (2006).

[2] H. Berns, A. Fischer, Microstructure of Fe-Cr-C hardfacing alloy with additions of Nb, Ti, B [J]. Materials Characterization **39** (2-5), 499-527 (1997).

[3] E.O. Correa, N.G. Alcântara, D.G. Tecco, et al., The relationship between the microstructure and abrasive resistance of a hardfacing alloy in the Fe-Cr-C-Nb-V system. Metallurgical and Materials Transactions A: Physical Metallurgy and Materials Science **38** (8),1671-1680 (2007).

[4] Jiang Jianmin, Xia Liming, He Dingyong, et al., The effect of niobium content on the microstructure and properties of Fe Cr C deposited metal [J]. China Surface Engineering **22** (5), 62-65 (2009).

[5] Pan Chuan, Wu Zhiwu, Wang Yishan, etc., The Role of Nb in High Chromium Cast Iron Surfacing Metal [J]. China Surface Engineering **25** (1), 104-109 (2012).

[6] Yang Ke, Gao Yuan, Yang, Kè, et al., Microstructure and wear resistance of Fe-Cr13-C-Nb hardfacing alloy with Ti addition. Wear B **376-377**, 1091-1096 (2017).

[7] Liu Zhengjun, Gou Jian, Jia Hua, et al., Micro-structure and wear resistance of Fe-Cr-C-B-Nb surfacing alloy. Journal of Welding **39** (3), 75-78 (2018).

[8] F. Huang, Z. Ren, W. Liu, et al., Effects of graphite additions on microstructures and wear resistance of Fe-Cr-C-Nb hardfacing alloys [J]. Materials Science **23** (3), 233-237 (2017).